

Processing of ground roll for the study of near-surface Rayleigh wave dispersion

Andrew Mills and Kris Innanen

ABSTRACT

In investigations of the generation of dispersion curves from shot records, it was noted that as receiver spacing increased, aliasing noise and other artefacts in the tau-p domain increased. This resulted in shear wave velocity dispersion curve “noise”, which masked the true dispersion curve. The purpose of this study is to test whether interpolation of ground roll in synthetic shot records can reduce the tau-p aliasing from sparsely sampled shot records, and as a result improve the generated dispersion curves.

Synthetic shot records are generated at varying receiver spacings, then two methods of processing are tested and compared. Processing of raw shot records to isolate ground roll followed by interpolation, and interpolation of raw shot records followed by processing to isolate ground roll. Dispersion spectrum noise is reduced or eliminated at low frequencies with both methods. However, when interpolation follows processing, the maximum detectable dispersion curve frequency is less than for the reverse process. This reverse process achieves an equivalent result to the original 10m receiver spacing dispersion spectra at frequencies below 35Hz.

INTRODUCTION

In Mills et al. (2016), initial modelling of surface wave dispersion was conducted, which produces clear dispersion curves with good resolution to high frequencies (80Hz). The above paper outlines methods of near surface characterization, specifically multichannel analysis of surface waves (MASW). A 2m receiver spacing is used for all models in that study, as a tight receiver spacing is typically used in MASW surveys, as small as 1m in Long and Donahue (2007) and Park et al., (2002). However, in exploration seismic surveys, it is uneconomical and unnecessary to sample so frequently, so larger receiver spacings are used. At receiver spacing equal to those seen in the 2011 experimental low frequency Hussar survey of 20m (Margrave et al., 2011), the aliasing noise is severe enough to mask the dispersion trend at any frequency. In the Hussar data, dispersion curve generation efforts are fruitless, and result in dispersion plots consisting almost entirely of noise. It is the goal of this report to explore the possibility of improving the resolution of dispersion spectra through interpolation of reflection survey scale seismic data to a denser receiver spacing. Synthetic shot records will be used to study dispersion curve generation, and processing methods to improve these. Shot records, and their associated dispersion spectra, will be compared for receiver spacing's of 20m and 10m. LNMO correction followed by 2D interpolation is used to resample the shot records, but other filtering methods are tested on the shot records to improve the resulting dispersion spectra.

THEORY

Dispersion and dispersion spectra

Shear wave dispersion spectra are generated for each shot record through several processes. First, the shot record $d(x, t)$ is Fourier transformed over t to $d'(x, \omega)$. This data is then tau-p transformed from $d'(x, \omega)$ to $d''(p, \tau)$. The discrete tau- p transform is described by equation 1 (Turner, 1990)

$$F(\tau, p) = \sum_{i=1}^n F(x_i, \tau + px_i) \quad (1)$$

Where:

n = number of seismic traces used in the transform,

x = horizontal space coordinate or position of the seismic trace,

t = two-way traveltime,

$\tau = p$ = zero offset intercept,

p = apparent slowness,

f = frequency,

$F(x, t)$ = amplitude at (x, t) in the standard seismic section, and

$F(\tau, p)$ = amplitude at (τ, p) in the tau- p domain.

This tau- p transform is performed over a range of slowness values, producing tau- p data with twice as many p traces as there were x traces. This data is then Fourier transformed over the time variable τ , producing $d'''(p, \omega)$. The phase velocities are then extracted by mapping slowness p to velocity, trace-by-trace. Computing the amplitude spectrum of the tau data yields the values of the frequencies (ω) (Yilmaz, 2015). Modelled dispersion spectra for the data are finally generated by plotting phase velocity vs frequency ω .

Often, tau- p transforms are utilized to filter out coherent noise such as ground roll, especially when this noise is spatially aliased (Turner, 1990). In this paper however, the tau- p transform is employed to isolate ground roll and extract near-surface dispersion curves.

Linear normal moveout correction

Linear normal moveout (LNMO) corrections apply a static shift to each trace, in order to flatten arrivals in shot records. The static shift is determined by the following,

$$LNMO \text{ Static Shift} = \frac{\text{Trace Offset}}{LNMO \text{ Velocity}} \quad (2)$$

Since there are multiple velocities and time-dips represented on a single shot record, these may be LNMO corrected independently. For a laterally heterogeneous near surface, the positive and negative offsets will also have different velocities and time-dips, resulting in

different correction being applied on either side of the source. A simpler and faster method which achieves similar results, is performing a single LNMO correction for an average LNMO velocity of the ground roll. This shifts the ground roll arrivals into a sub-horizontal orientation, which improves the 2D interpolation.

Interpolation

The interpolation used for this study is a 2D trace interpolation, 2DIntr in GEDCO Vista, which operates in the frequency-wave number (FK) domain (GEDCO, 2013). The LNMO corrected shot records are input into the interpolation algorithm, which runs over the entire dataset. Within this data, the events of interest, ground roll, are mostly sub-horizontal and parallel, but non-parallel and angled events are handled by the 2 dimensionality of the interpolation. Initially in the interpolation, an operator is built from traces in the FK domain, and the input data is deconvolved with this operator to create new traces evenly spaced between existing traces. This halves the receiver spacing for the interpolated data. After the initial approximation of the interpolated traces has been created through deconvolution, the process iterates a set number of times. For this study, 10 iterations are used, as further iterations fail to improve the result significantly.

From the Vista documentation: Data is then transformed into the frequency-wave number (FK) domain. At this step, the FK spectrum is the result of convolution of the full data spectrum with a Fourier transformation of the sampling operator (1 or 0 for existing or missing traces). This spectrum distortion is also known as spectrum “leakage”, which means that each original spectrum component affects others and components with stronger amplitudes have more impact especially on the nearest components.

At each iteration, spectrum components larger than the threshold (10%) are selected and the components which are also local maximums are accumulated in the output spectrum. After an inverse FK transformation, the components from all previous iterations are subtracted from the input frequency spectrum, which will then be the input for the next iteration. Thus, by subtracting the strongest components, we reduce the strongest distortion of weaker components due to “leakage”.

The threshold is reduced at each step of the procedure from the defined value to zero, which also allows the updating of previously estimated components in order to reduce inaccuracy of the initial estimation of spectrum components at later iterations.

DATA AND RESULTS

Initially synthetic shot records are created with 20m and 10m receiver spacing, over the same geological model, and dispersion spectra are generated for these. The 10m spacing shot record and spectra will be the standard that we attempt to recreate from the more sparsely sampled 20m shot record. First, the 20m shot record will be LNMO corrected using an average ground roll velocity.

Synthetic modelling

The geologic V_p , V_s , and ρ models are built in MatLab, and are 5000m wide by 2500m deep. Models represent a complex near surface in the shallowest 100m, including a vertical

discontinuity at $x=2500\text{m}$ offsetting the three near surface layers, with three deeper layers to a maximum reflector depth of 1510m (Figure 1).

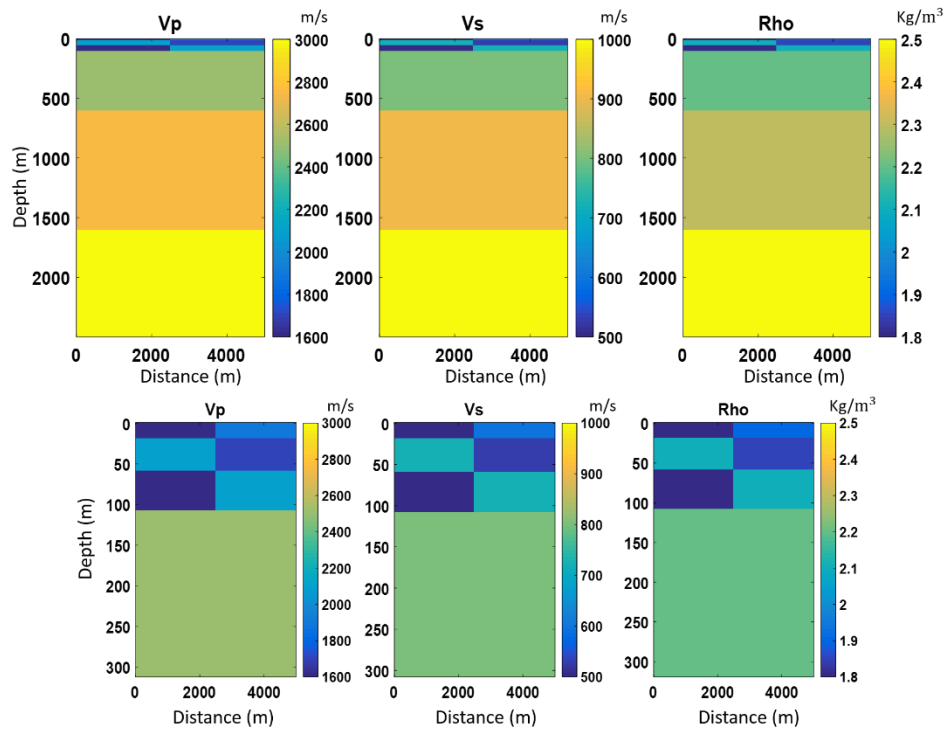


FIG. 1. Geologic models used for synthetic modelling. Top: Full model. Bottom: Near surface zoom.

The synthetic modelling is carried out using SOFI2D, a 2D finite difference elastic modelling engine. The top of the model is set as a free surface, meaning that Rayleigh waves can be generated and recorded, which is necessary for this dispersion study (Mills et al., 2016). Absorbing boundary conditions are on the sides and bottom of the model, however some artificial reflections from these boundaries still appear. An explosive point source is placed at 5m depth, at $x=2500\text{m}$. A Fuchs-Muller minimum-phase wavelet with a central frequency of 12 Hz is used for the source. Receivers are placed at 5m depth across the model at varying receiver spacing. Once SOFI2D has run using the input models and specified receiver locations, a 2 second shot record is generated with a time sampling rate of 1ms . These shot records can then be analyzed in seismic unix (SU) format in Vista or Matlab.

Initial data

The initial shot record which will be processed to extract dispersion spectra, is a single shot at the centre of the above model (Figure 1), with 20m receiver spacing (Figure 2, Left). This shot record contains reflection events, which are dimly visible, direct arrivals and refractions, and high amplitude ground roll as the most steeply dipping arrivals. In Figure 2 (Right) the tau-p transformed data is shown. It is from the tau-p data that the dispersion spectra are created, so it is beneficial to have clear data in the tau-p domain. There are a number of details obfuscating the ground roll components of this data, as shown in Figure

3. Through multiple processing steps, we will attempt to filter and remove these parts of the data, enhancing the signal from the ground roll.

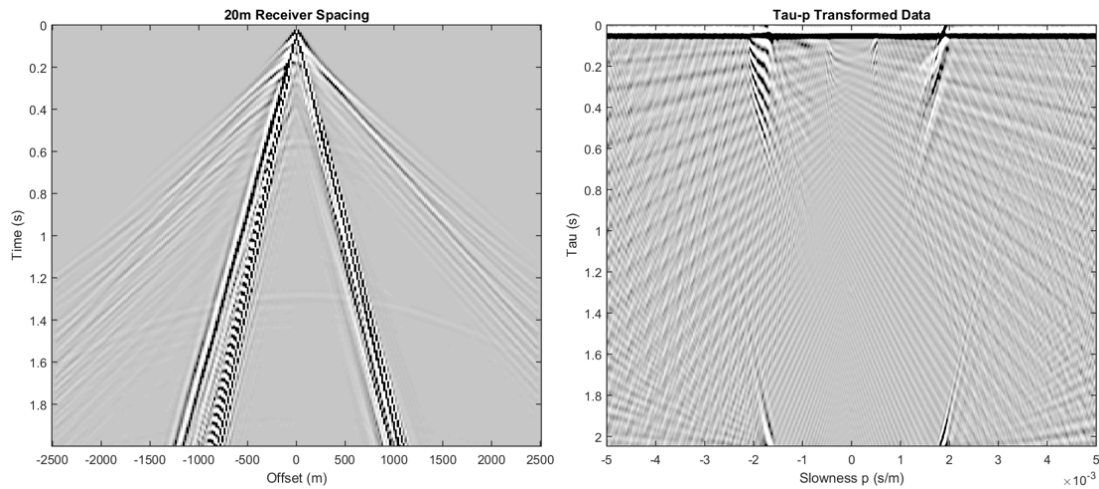


FIG. 2. Left: Shot record with 20m receiver spacing. Right: Tau-p transformed shot record data.

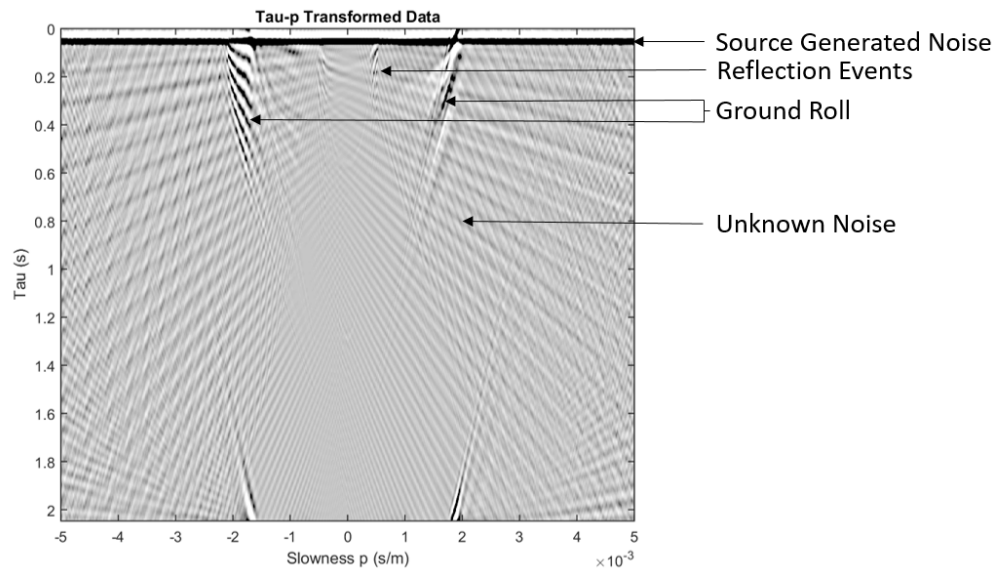


FIG. 3. Same Tau-p data as FIG.2. right, with labelled components.

Because the shot is in the centre of the asymmetric model, with different model properties on either side of the shot, the dispersion spectra consists of two different components. These are shown in Figure 4, where the top curve represents positive offset data (Positive phase velocity) and the bottom curve represents negative offset data (Negative phase velocities). In these dispersion spectra, the fundamental mode is quite visible to 30 Hz, and higher modes of dispersion are visible in the bottom curve between 20 Hz and 45 Hz.

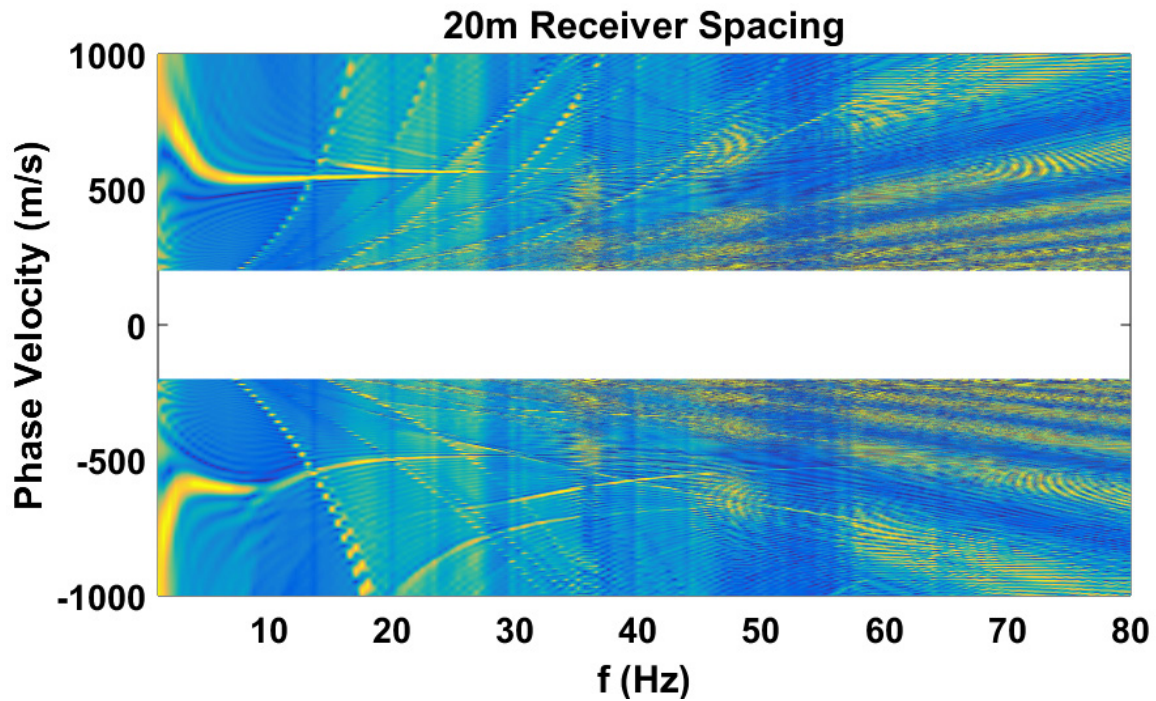


FIG. 4. Shear wave dispersion spectra from the 20m receive spacing shot record. The thick yellow curve is the fundamental mode of the dispersion. Top: positive offset dispersion. Bottom: Negative offset dispersion.

As stated earlier, the goal of this paper is to improve the resolution of these dispersion spectra through processing and interpolation of this original 20m receiver spacing shot record. To begin, a 10m receiver spacing synthetic shot record was produced over the same geological models as before (Figure 5). It can be seen in the tau-p domain data (Figure 5: right) that the denser spatial sampling rate results in better resolution of the ground roll signals than in Figure 2 (right). The linear noise originating at (0,0) in the tau-p domain has lower amplitude relative to the ground roll. As a result of this, the generated dispersion spectra from this shot record (Figure 6) is clearer, and the fundamental mode of dispersion is visible up to 40 Hz.

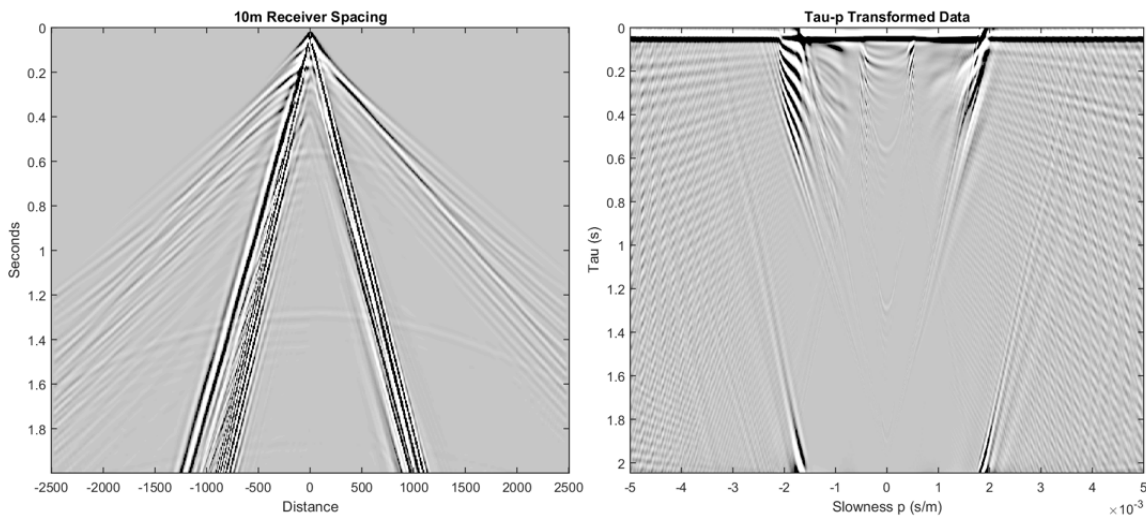


FIG. 5. Left: Shot record with 10m receiver spacing. Right: Tau-p transformed shot record data.

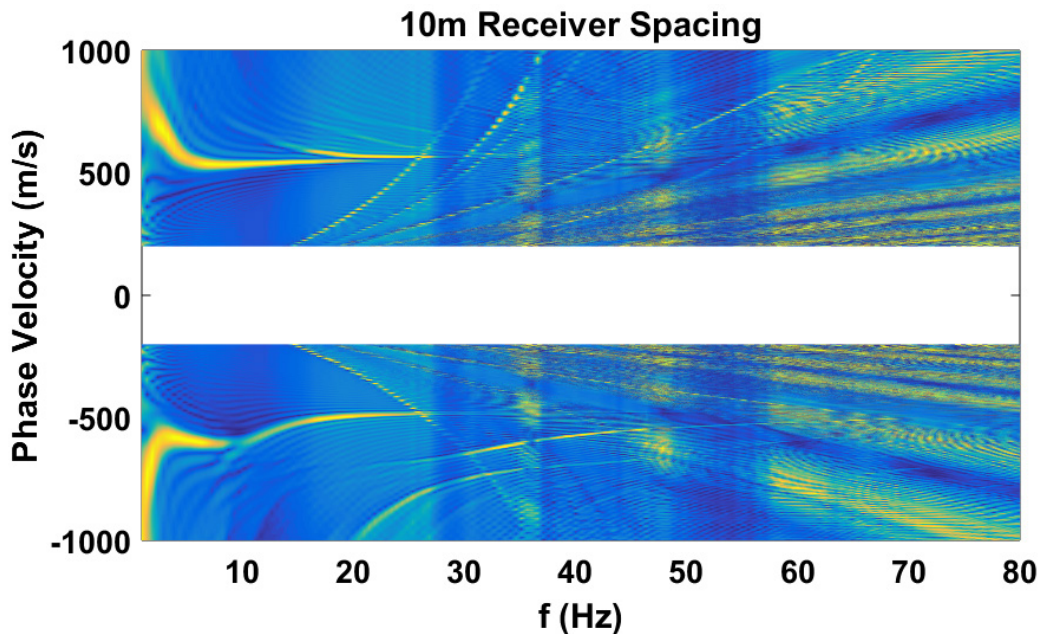


FIG. 6. Dispersion spectra from the 10m receiver spacing shot record. Note the better resolution of the fundamental dispersion mode compared to FIG. 4, and fewer artefacts at low frequencies.

Processing and results

Method 1: Processing followed by interpolation

First, some simple processing will be applied to the raw 20m receiver spacing shot record in an attempt to improve the dispersion spectra. Since we are interested in surface waves and ground roll, isolating the ground roll in the shot records should reduce the effect of other events, improving the spectra. In early tests, it was observed that muting reflections and refractions in the shot record resulted in slightly cleaner dispersion curves, removing some of the linear noise at higher frequencies. This was attempted in a more sophisticated way by applying an FK filter to the raw 20m shot record to remove the reflections and

much of the refracted arrivals. The FK filtered shot record and its tau-p domain data are shown in Figure 7. The produced dispersion curves from this step (Figure 8) are less resolvable than those from the raw 20m receiver spacing data. There are new noise artefacts from 20-30 Hz, which obscures the previously visible fundamental mode dispersion curve. Muting the remaining refractions and events outside the ground roll cone results in no further improvement of the dispersion spectra.

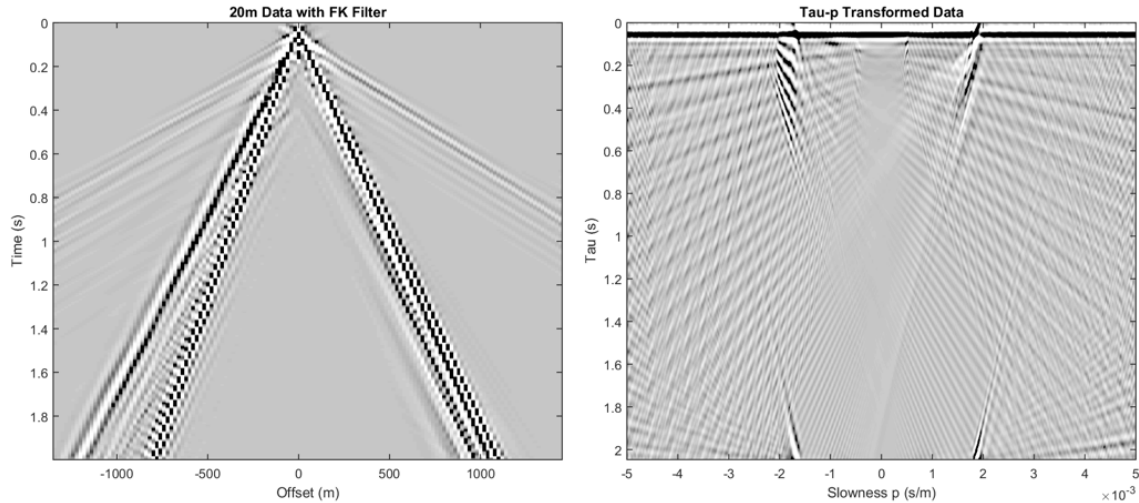


FIG. 7. FK filtered data (Left) and its tau-p domain data (Right).

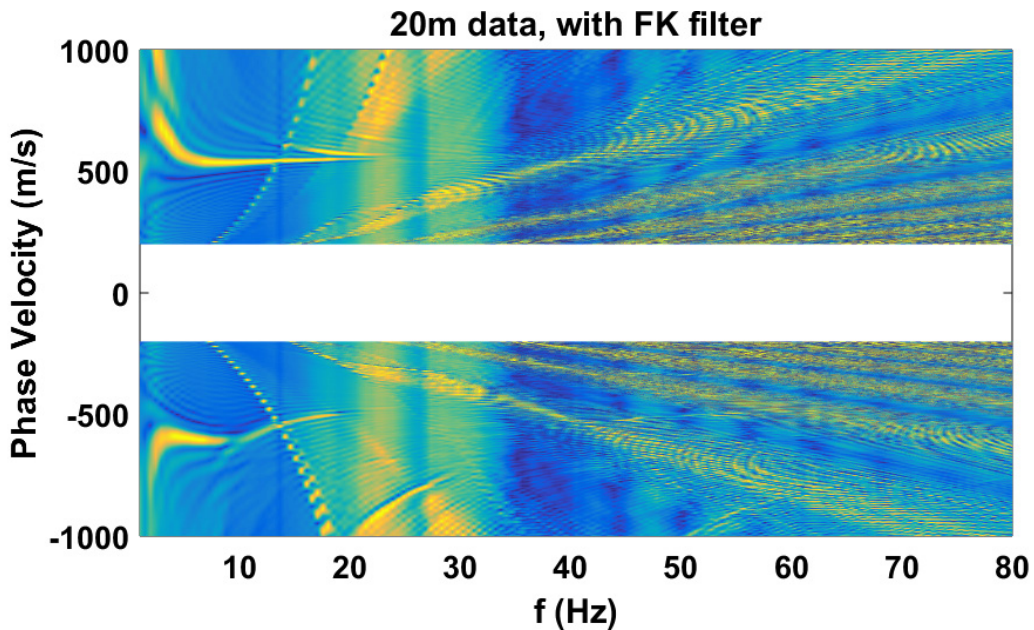


FIG. 8. Dispersion spectra from data in Figure 7. Note lower quality compared to the raw 20m spectra.

Finally, a 2D trace interpolation is performed on the 20m receiver spacing shot record, after FK filtering and refraction muting. This halves the receiver spacing of the interpolated shot record to 10m, the same as the record we are attempting to recreate, allowing a direct comparison.

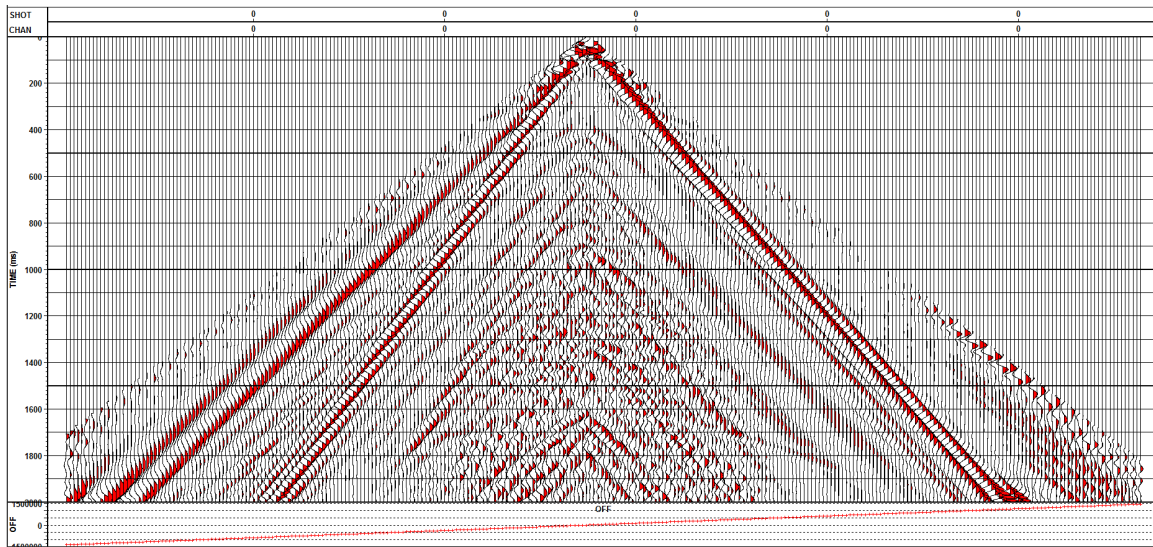


FIG. 9. 20m to 10m interpolation, with AGC applied for viewing. Interpolation preceded by FK filtering and muting of refractions.

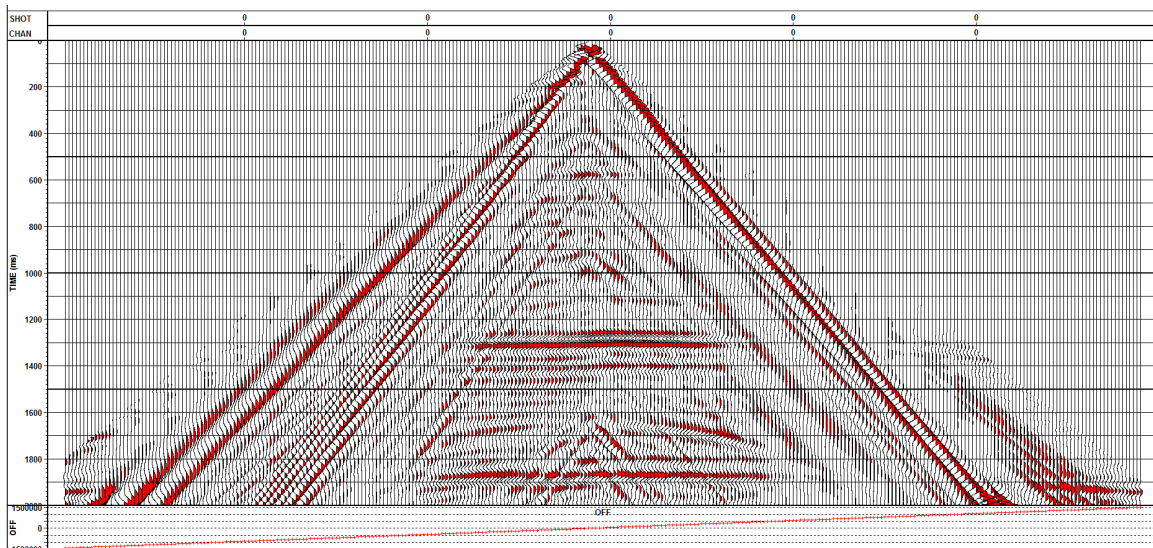


FIG. 10. Original 10m receiver spacing data. View restricted to offsets containing ground roll. Refractions muted to same window as interpolation. AGC has been applied for viewing.

The interpolation (Figure. 9) has produced a ground roll data that closely resembles that of the original 10m data (Figure. 10). The main difference is visible in the centre of the shot record, where reflections present in the original have been removed by FK filtering. Another major difference is that some ground roll events at later times (>1000ms) are missing after the interpolation. This could be due to relative amplitude differences from adjacent events.

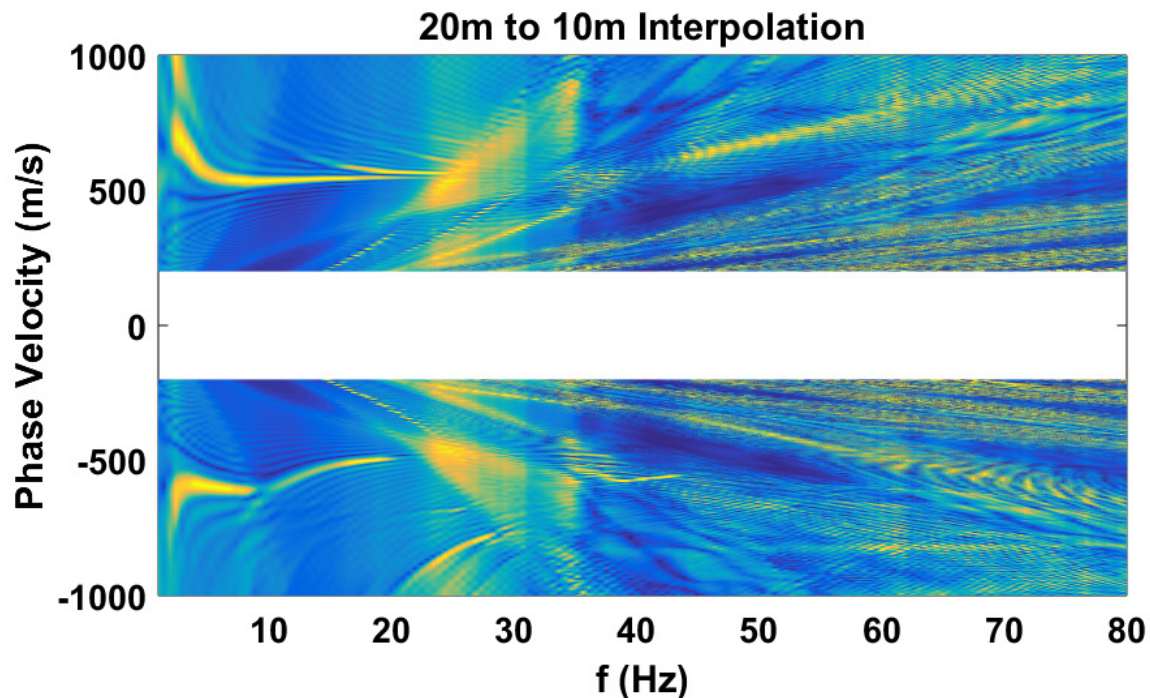


FIG. 11. Dispersion spectrum from the 20m to 10m interpolation in Figure 9.

In the dispersion spectra (Figure 11) for the interpolated shot record, it can be seen that noise is reduced significantly at frequencies below 35 Hz. However, the fundamental mode dispersion curves are no more visible than in the FK filtered spectra. Despite this, since the dispersion curves are much less obscured by noise below 30 Hz, accurate picking of the dispersion curve should be improved. Note that before generating the dispersion spectrum for all cases, any zero traces (all traces outside the LNMO correction velocity wedge) are deleted from the shot records, as they result in noise in the dispersion spectra.

Method 2: Interpolation followed by processing

As an alternative to processing the original shot record and then interpolating, we can interpolate the shot record to 10m receiver spacing, and then process it to enhance the ground roll signal. The same interpolation procedure is followed as before: the raw shot record is LNMO shifted, the interpolation is performed, and the LNMO correction is reversed. This results in a 10m receiver spacing shot record, with muted refractions and offsets outside the ground roll signals. The interpolation in this case is a closer match to the original 10m data than the previous attempt. The interpolated ground roll signals are nearly a perfect match to the original, with only slight amplitude differences. The ground roll events that were not correctly interpolated in Figure 9 are present in this interpolation. The main issue is the incorrect interpolation of reflection events in the centre of the shot record. This is due to these events not being flattened by the LNMO shift before interpolation, resulting in a time shift and amplitude error after interpolation and reverse LNMO correction.

The produced dispersion spectrum from this interpolation is shown in Figure 14. This spectrum is significantly improved over the original 20m receiver spacing dispersion

spectrum (Figure 4). This is an important result, as it shows that spatial sampling rate alone is responsible for many of the artefacts seen in the original dispersion spectra.

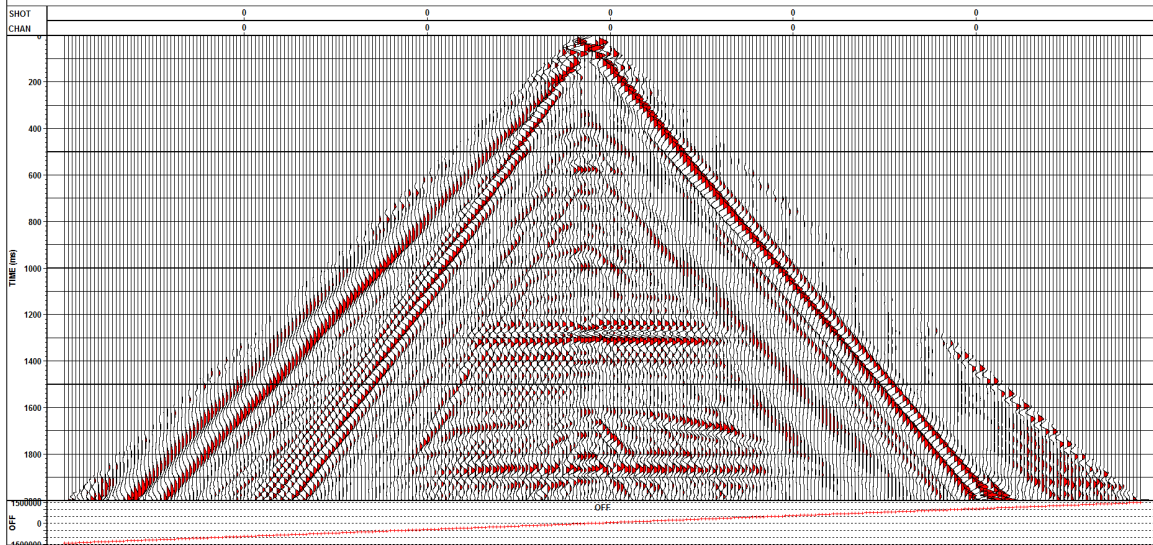


FIG. 12. 20m to 10m interpolation, with AGC applied for viewing.

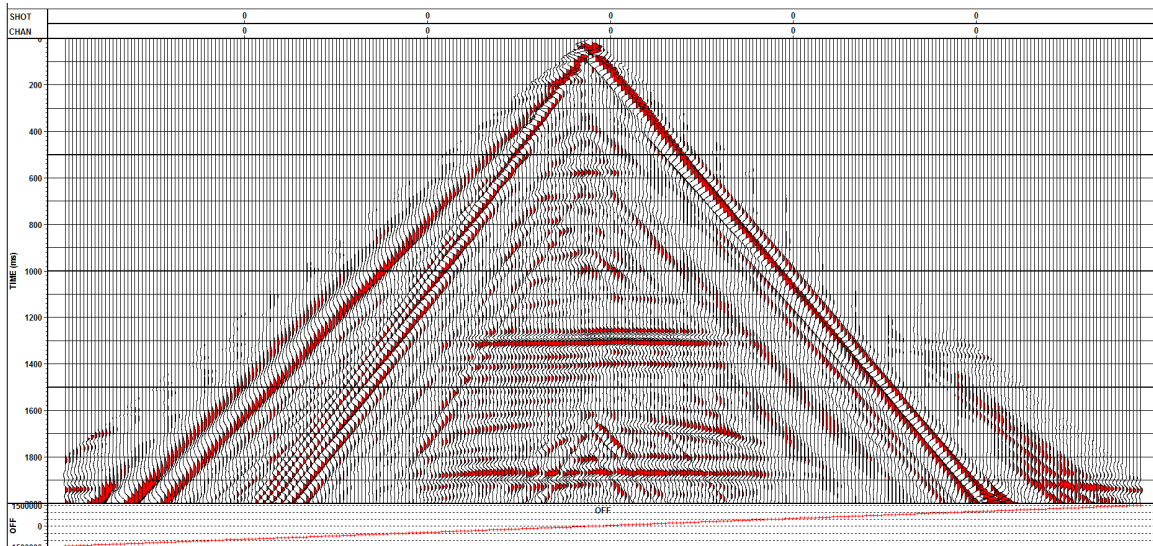


FIG. 13. Original 10m receiver spacing data. View restricted to offsets containing ground roll. Refractions muted to same window as interpolation. AGC has been applied for viewing.

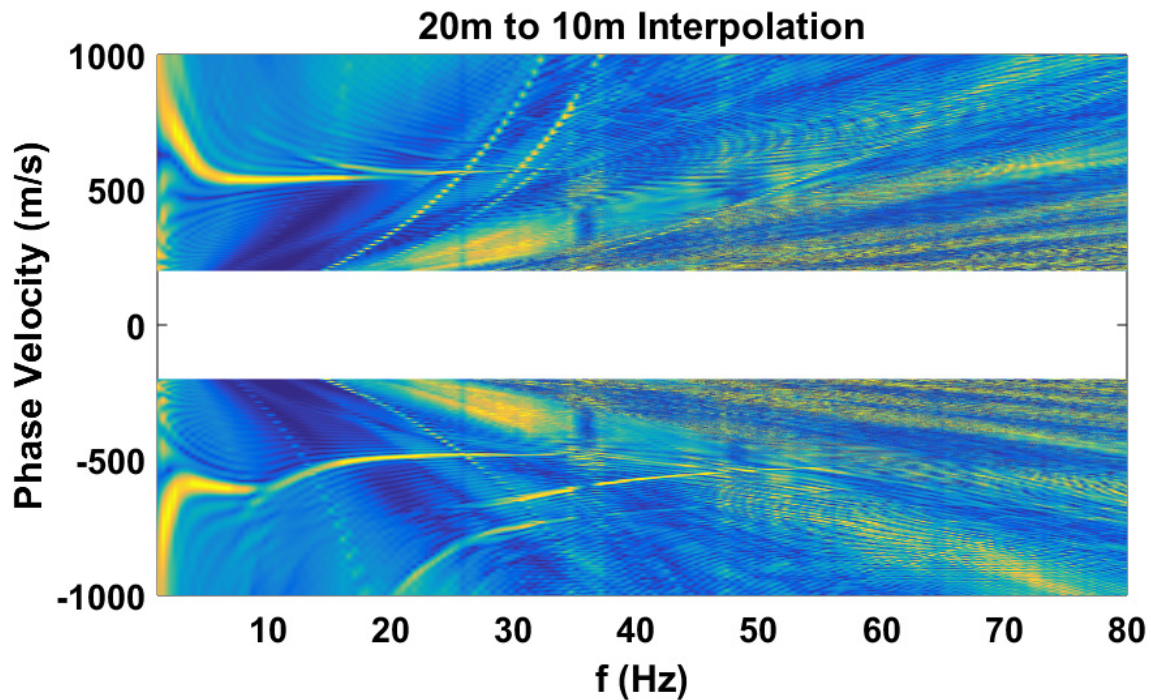


FIG. 14. Dispersion spectrum from the 20m to 10m interpolation in Figure 12.

Despite this improvement, there still remains an artefact that truncates at 20Hz, -1000m/s. Quality of the curves also suffer above 40Hz. We can follow the interpolation up with similar processing that was applied to the shot records in the previous section. Muting refractions and direct arrivals is unnecessary, as the reverse LMNO correction mutes these events. We can proceed with FK filtering the 20m to 10m interpolated shot record (Figure 12). This shot record and its FK spectrum are shown in Figure 15. A similar FK filter to the one used in method 1 is applied, filtering data in the centre of the spectrum. There is significant aliasing present in this case, that is not filtered out. This aliasing was filtered in different tests, but there was no significant improvement of dispersion spectra.

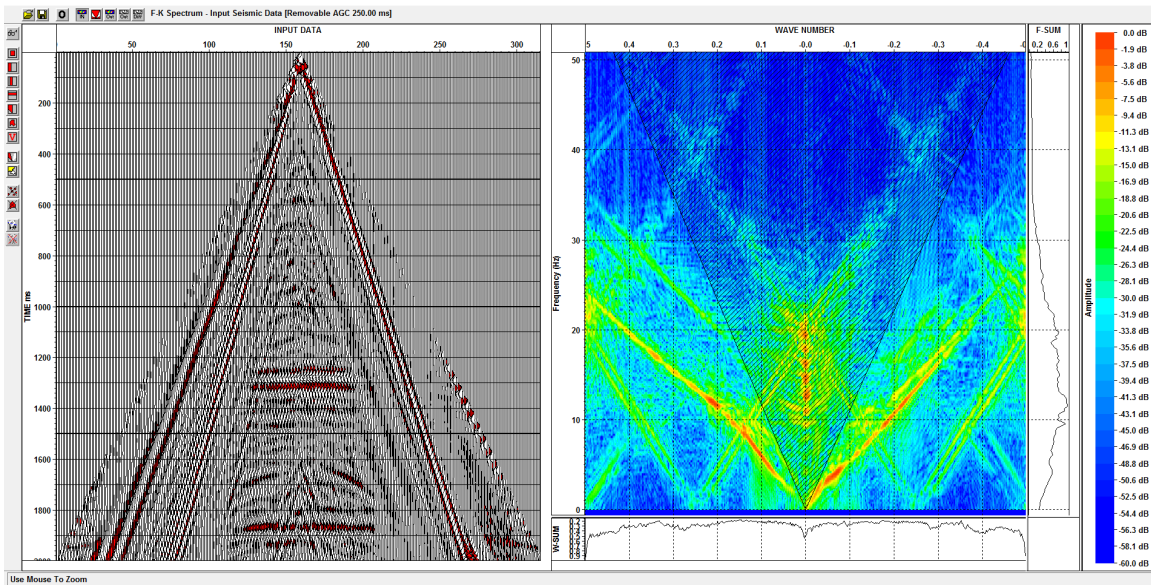


FIG. 15. Input data (Figure12) (Left) and it's FK spectrum with the filter used (Right).

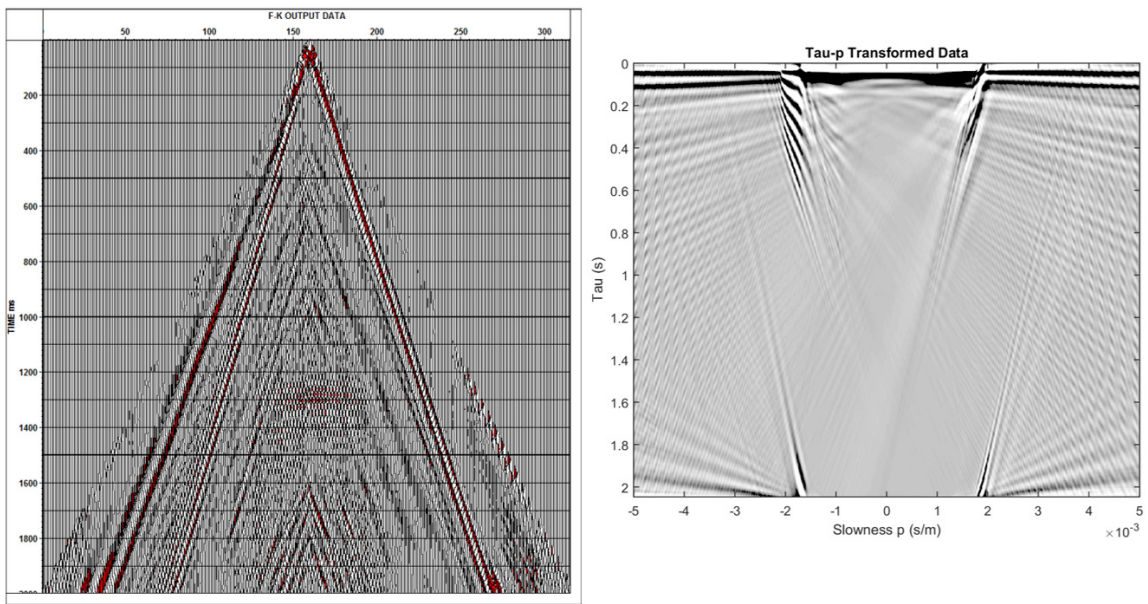


FIG. 16. FK filtered shot record, and the tau-p domain data.

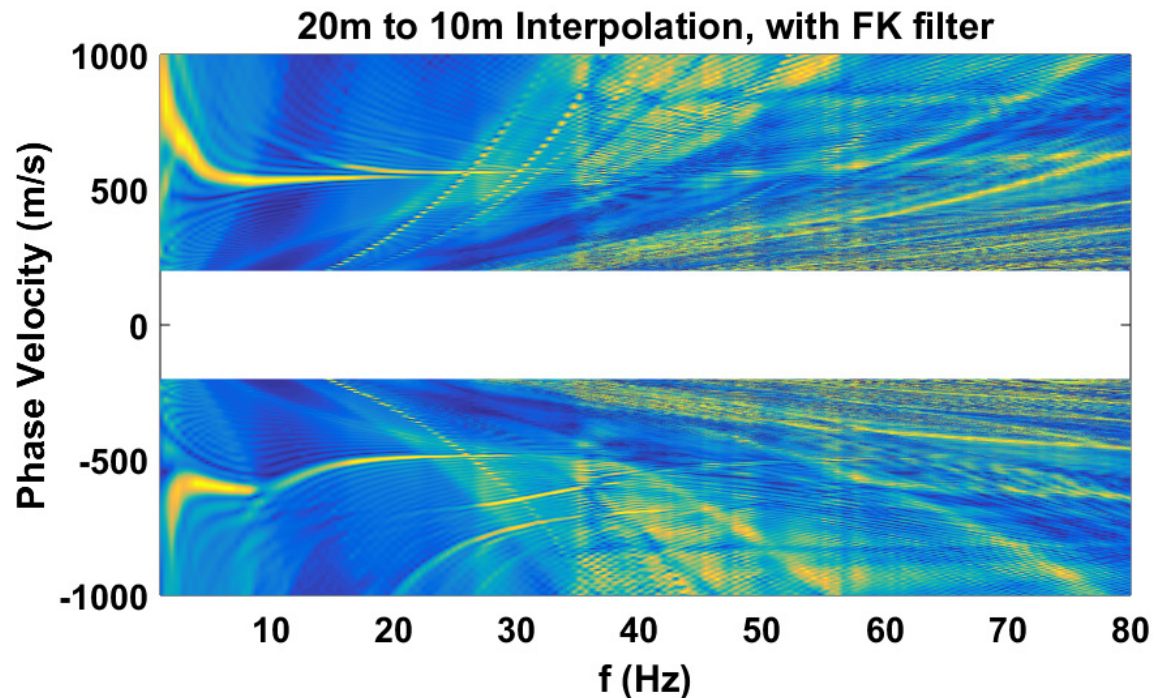


FIG. 17. Dispersion spectrum for the interpolated and FK filtered data in Figure 16(Left).

The dispersion spectrum (Figure 17) is now slightly clearer than after the interpolation, and very similar to the original 10m dispersion spectrum (Figure 6) up to 35 Hz. Below 35 Hz, the dispersion curve (Yellow) is clear, unobstructed, and uncrossed by other events. The curves are continuous and traceable to 35 Hz, and are even brighter from 30-35 Hz than in the original. This demonstrates that with processing, we are able to meet and even exceed the quality of dispersion spectra produced from data with twice as dense receiver spacing. With further interpolation and filtering, it is likely these spectra can be improved even further to match those of tighter receiver spacing spectra.

DISCUSSION AND FUTURE WORK

Two methods of improving resolution of dispersion curves were tested. Method 1 consisted of processing 20m receiver spacing shot records, followed by interpolation to 10m receiver spacing. Method 2 involved interpolating from 20m to 10m, followed by processing.

Initial FK filtering of the shot records in method 1 removed some noise from dispersion spectra, but added noise that obscured the curve at higher frequencies. This noise persisted through interpolation, resulting in clean spectra <20-25 Hz, but discontinuation of curves above this. In method 2, interpolation removed some noise, and the following FK filtering removed additional artefacts, resolving the dispersion curves well up to 35 Hz.

Applying alternative filtering in method 1 may result in less noise being produced in the resulting dispersion spectra, which after interpolation would likely produce better results than method 2. However, in the process followed here, method 2 achieved better results, even improving the frequency range of the dispersion curves by up to 5 Hz over the original 10m spacing spectra.

To continue on with this work, further interpolations can be performed to interpolate from 20m receiver spacing to 2.5m or less to replicate a MASW survey. This will involve determining when filtering and muting should be performed, and whether it should be repeated between interpolations or after the last interpolation. A dispersion curve picking tool is being developed to test how well the curves can be picked, and find where the picking fails. Once dispersion curves are picked, we will be able to invert for 1D shear wave velocities for each shot record along the survey line, and produce shear wave velocity profiles.

CONCLUSIONS

MASW surveys are conducted using very dense receiver spacing (1-2m), while this is uneconomic for larger scale exploration surveys which use receiver spacings in the 15-25m range. Shear wave velocity dispersion curves produced for denser receiver spacings are very clear, with few or no artefacts obscuring the curve, while noise obscures much of the curve for greater receiver spacings. Through interpolation, FK filtering, and muting, we attempted to improve the resolution of these dispersion curves to match those produced from denser sample spacings.

20m and 10m receiver spacing shot records were produced by synthetic modelling over a model with a complex near surface. Dispersion spectrums were produced for each of these, with the goal of reproducing the 10m spectrum through processing of the 20m shot record. Two methods were tested: Method 1 consisted of processing followed by interpolation, and method 2 consisted of the reverse, interpolation followed by processing.

The processing involved FK filtering shot records to remove reflections, muting of refractions and direct arrivals, and 2D trace interpolation to decrease receiver spacing. To achieve an accurate interpolation, it was necessary to flatten ground roll events as much as possible through LNMO correction prior to interpolation, using an average ground roll velocity, and reversing this after interpolation.

Method 1, processing followed by interpolation, produced dispersion spectra with curves resolvable up to 25 Hz. Method 2, interpolation followed by processing, produced dispersion spectra with curves resolvable up to 35 Hz. In method 2, resolution of the curves was improved over the original 10m spectra between 30-35 Hz. When method 2 is followed, more sparsely sampled data can be interpolated and processed, to match the quality of data acquired with closer receiver spacing. This demonstrates that sparser receiver spacings can be used in the initial survey to reduce costs, and processed to a higher sample rate as needed to acquire dispersion data.

ACKNOWLEDGMENTS

The authors thank the sponsors of CREWES for continued support. This work was funded by CREWES industrial sponsors and NSERC (Natural Science and Engineering Research Council of Canada) through the grant CRDPJ 461179-13.

REFERENCES

- GEDCO, 2013, 2D trace interpolation, GEDCO Vista program documentation, Version 2013.0.0.
- Long, M. and Donahue, S., 2007, In situ shear wave velocity from multichannel analysis of surface waves (MASW) tests at eight Norwegian research sites, *Canadian Geotechnical Journal*, **44**, 533-544.
- Margrave, G.F., Mewhort, L., Phillips, T., Hall, M., Bertram, M.B., Lawton, D.C., Innanen, K., Hall, K.W., and Bertram, K., 2011, The Hussar low-frequency experiment, CREWES research reports, Volume **23**.
- Mills, A., Cova, R., and Innanen, K., 2016, Surface wave modelling and near surface characterization background, CREWES research reports, Volume **28**.
- Park, C.B., Miller, D.M., and Miura, H., 2002, Optimum field parameters of an MASW survey, SEG-J Expanded Abstracts.
- Turner, G., 1990, Aliasing in the tau- p transform and the removal of spatially aliased coherent noise, *Geophysics*, **55**, No. 11, 1496-1503.
- Yilmaz, O. 2015, *Engineering seismology with applications to geotechnical engineering*, Society of Exploration Geophysicists.